Analysis of velocity-components decoupled projection method for the incompressible Navier–Stokes equations

Xiaomin PAN [1]

1) *Department of Computational Science and Engineering, Yonsei University, Seoul 03722, KOREA*

We study the temporal accuracy and stability of the velocity-components decoupled projection method (VDPM) for fully discrete incompressible Navier–Stokes equations. In particular, we investigate the effect of three formulations of the nonlinear convection term, which include the advective, skew-symmetric, and divergence forms, on the temporal accuracy and stability. Second-order temporal accuracy of the VDPM for both velocity and pressure is verified by establishing global error estimates in terms of a discrete l^2-norm. Considering the energy evolution, we demonstrate that the VDPM is stable when the time step is less than or equal to a constant. Stability diagrams, which display the distributions of the maximum magnitude of the eigenvalues of the corresponding amplification matrices, are obtained using von Neumann analysis. These diagrams indicate that the advective form is more stable than the other formulations of the nonlinear convection term. Numerical tests are performed in order to support the mathematical findings involving temporal accuracy and stability, and the effects of the formulations of the nonlinear convection term are analyzed. Overall, our results indicate that the VDPM along with an advective discrete convection operator is almost unconditionally stable, second-order accurate in time, and computationally efficient because of the non-iterative solution procedure in solving the decoupled momentum equations.

1 BASIC PRINCIPLE OF THE PROJECTION METHOD

We consider incompressible viscous flow in a bounded domain Ω in $\mathbb{R}^3$ with boundary $\partial\Omega$ over a finite time interval $[0, T]$. The time-dependent Navier–Stokes equations and continuity equation for incompressible viscous flows are:

$$\frac{\partial \mathbf{u}}{\partial t} + c_\beta(\mathbf{u}, \mathbf{u}) = -\nabla p + \frac{1}{Re}\nabla^2 \mathbf{u} \tag{1}$$

$$\nabla \cdot \mathbf{u} = 0 \tag{2}$$

and are subject to suitable boundary conditions on $\partial\Omega$. Here, $\mathbf{u} = (u_1, u_2, u_3)^T$ denotes velocity, p indicates pressure, Re is the Reynolds number, and $c_\beta(\cdot, \cdot)$ represents the continuous nonlinear convection operator. In this paper, we consider three formulations of the nonlinear convection term $c_\beta(\mathbf{u}, \mathbf{u})$ in the momentum equation. The formulations can be defined as

$$(c_\beta(\mathbf{u}, \mathbf{u}))_i := (1 - \beta)u_j\frac{\partial u_i}{\partial x_j} + \beta\frac{\partial u_j u_i}{\partial x_j} \quad \text{for} \quad \beta = 0, 1/2, \text{and } 1 \tag{3}$$

in which $c_0(\cdot, \cdot)$, $c_{1/2}(\cdot, \cdot)$, and $c_1(\cdot, \cdot)$ represent advective, skew-symmetric, and divergence forms, respectively, x_j are the Cartesian coordinates, and the subscripts denote direction.

We use a staggered MAC mesh for spatial discretization:

$$\frac{\mathbf{u}^{n+1} - \mathbf{u}^n}{\triangle t} = -\frac{1}{2}\left(\mathcal{C}_\beta\left(\mathbf{u}^{n+1}, \mathbf{u}^{n+1}\right) + \mathcal{C}_\beta\left(\mathbf{u}^n, \mathbf{u}^n\right)\right) + \frac{1}{2Re}\left(\mathcal{L}\mathbf{u}^{n+1} + \mathcal{L}\mathbf{u}^n\right)$$
$$-\mathcal{G}p^{n+1/2} + \mathbf{mbc}^{n+1/2} \tag{4}$$

$$\mathcal{D}\mathbf{u}^{n+1} = cbc^{n+1} \tag{5}$$

where discrete operators $\mathcal{C}_\beta$, $\mathcal{L}$, $\mathcal{G}$, and $\mathcal{D}$ are defined for convection, Laplacian, gradient, and divergence operators, respectively. Three discrete convection operators, such as $\mathcal{C}_0$, $\mathcal{C}_{1/2}$, and $\mathcal{C}_1$, are considered based on the respective advective, skew-symmetric, and divergence forms of the continuous convection operator in (3). The corresponding discrete operators for $\mathbf{u}^n$ and $\mathbf{v}^n \in H^1(\Omega_h)^3$ can be defined as

$$\mathcal{C}_\beta\left(\mathbf{u}^n, \mathbf{v}^n\right) := (1 - \beta)\mathbf{u}^n \cdot \mathcal{G}\mathbf{v}^n + \beta\mathcal{D}\left(\mathbf{u}^n \otimes \mathbf{v}^n\right) \text{ for } \beta = 0, 1/2, \text{ and } 1. \tag{6}$$

For simplicity, we introduce discrete operator $\mathcal{N}$ for the linearized form of the nonlinear convection term:

$$\mathcal{N}\left(\mathbf{u}^{n+1}\right) = \frac{1}{2}\left(\mathcal{C}_\beta\left(\mathbf{u}^n, \mathbf{u}^{n+1}\right) + \mathcal{C}_\beta\left(\mathbf{u}^{n+1}, \mathbf{u}^n\right)\right). \tag{7}$$

The complete procedure of the projection method presented by Kim et al. [1] can be summarized as follows:

$$\mathcal{A}\delta\mathbf{u}^{*,n+1} = \mathbf{R} \tag{8}$$

$$\mathbf{u}^{*,n+1} = \mathbf{u}^n + \delta\mathbf{u}^{*,n+1} \tag{9}$$

$$\mathcal{D}\mathcal{G}\left(\delta p^{n+1/2}\right) = \frac{1}{\triangle t}\mathcal{D}\mathbf{u}^{*,n+1} - \frac{1}{\triangle t}cbc^{n+1} \tag{10}$$

$$p^{n+1/2} = p^{n-1/2} + \delta p^{n+1/2} \tag{11}$$

$$\mathbf{u}^{n+1} - \mathbf{u}^{*,n+1} = -\triangle t\mathcal{G}\delta p^{n+1/2}. \tag{12}$$

in which $\mathcal{A} = \frac{1}{\triangle t}(\mathcal{I} + \triangle t(\mathcal{N} - \frac{1}{2Re}\mathcal{L}))$, $\mathbf{r}^n = \frac{1}{\triangle t}\mathbf{u}^n + \frac{1}{2Re}\mathcal{L}\mathbf{u}^n - \mathcal{G}p^{n-1/2}$, and $\delta p^{n+1/2} = p^{n+1/2} - p^{n-1/2}$. Note that $\mathbf{r}^n$ only relates to the information at the previous time level. Here $\mathbf{u}^{*,n+1}$ denotes the intermediate velocity, $\mathcal{I}$ is the identity matrix, and $\delta\mathbf{u}^{*,n+1} = \mathbf{u}^{*,n+1} - \mathbf{u}^n$. Because the intermediate velocity components are coupled, we must use an iterative procedure in order to solve $\delta\mathbf{u}^{*,n+1}$ in (8). The corresponding system matrix, $\mathcal{A}$, is given by

$$\mathcal{A} = \frac{1}{\triangle t}\begin{pmatrix} \mathcal{I} + \triangle t\mathcal{M}_{11} & \triangle t\mathcal{M}_{12} & \triangle t\mathcal{M}_{13} \\ \triangle t\mathcal{M}_{21} & \mathcal{I} + \triangle t\mathcal{M}_{22} & \triangle t\mathcal{M}_{23} \\ \triangle t\mathcal{M}_{31} & \triangle t\mathcal{M}_{32} & \mathcal{I} + \triangle t\mathcal{M}_{33} \end{pmatrix} \tag{13}$$

in which $\mathcal{M}_{ij}(i, j = 1, 2, 3)$ is a sub-matrix of $\mathcal{M}(\cdot) = \mathcal{N}(\cdot) - \frac{1}{2Re}\mathcal{L}(\cdot)$. The entire procedure (8)–(12) is called the velocity-components coupled projection method (VCPM).

In order to avoid the iterative procedure in (8), we apply a block LU decomposition along with approximate factorization technique to $\mathcal{A}$ for decoupling the velocity difference $\delta\mathbf{u}^{*,n+1}$, which produces the VDPM. Here, we define the numerical solutions $\mathbf{u}_d^{n+1} \in H^1(\Omega_h)^3$ and $p_d^{n+1/2} \in H^1(\Omega_h)$ of the VDPM at $(n + 1)\triangle t$ with intermediate velocity, $\mathbf{u}_d^{*,n+1} = (u_{d,1}^{*,n+1}$

$, u_{d,2}^{*,n+1}, u_{d,3}^{*,n+1})^T \in H^1(\Omega_h)^3$, in order to distinguish the numerical solutions obtained from the VCPM and VDPM. Here, $H^1(\Omega_h)$ denotes the space of functions:

$$H^1(\Omega_h) = \{\chi : \|\mathcal{G}\chi\|_{\Omega_h} < \infty\} \tag{14}$$

where χ is an edge-centered or cell-centered function in domain Ω_h. The discrete l^2-norm $\| \ \|_{\Omega_h}$ corresponds to a discrete inner product:

$$\langle \mathbf{u}, \mathbf{v} \rangle_{\Omega_h} = h^3 \sum_{m=1}^{M} u_m : v_m \tag{15}$$

where $\mathbf{u} = (u_1, \cdots, u_M)^T$, $\mathbf{v} = (v_1, \cdots, v_M)^T$, and : represents the Frobenius inner product. Note that the functions u_m and v_m ($m = 1, \cdots, M$) are edge-centered or cell centered. Accordingly, we have

$$\mathcal{A}_d = \frac{1}{\triangle t}\left(\mathcal{I} + \triangle t\left(\mathcal{N}_d - \frac{1}{2Re}\mathcal{L}\right)\right) \quad \text{and} \quad \mathcal{M}_d(\cdot) = \mathcal{N}_d(\cdot) - \frac{1}{2Re}\mathcal{L}(\cdot) \tag{16}$$

where $\mathcal{N}_d(\mathbf{u}_d^{n+1}) = \frac{1}{2}(\mathcal{C}_\beta(\mathbf{u}_d^n, \mathbf{u}_d^{n+1}) + \mathcal{C}_\beta(\mathbf{u}_d^{n+1}, \mathbf{u}_d^n))$. Applying the block LU decomposition along with approximate factorization and approximate factorization for each direction enable us to solve (8)–(12) efficiently.

2 TEMPORAL ORDER OF ACCURACY

Some hypotheses are needed to proceed.

- (H1), we assume a uniform boundedness within a finite time. If we consider the process up to time T, we can assume that $\|\mathbf{u}^n\|_{\Omega_h} < C$ and $\|p^{n-1/2}\|_{\Omega_h} < C$ for $n\triangle t < T$. Here, C is a given constant.

- (H2), we assume $\mathcal{C}_\beta$ is a Lipschitz operator with constant $C_{\mathcal{C}_\beta}$. Therefore, given uniform bounded $\|\mathbf{u}\|_{\Omega_h}$, $\|\mathbf{v}\|_{\Omega_h}$, $\|\mathbf{u}_1\|_{\Omega_h}$, and $\|\mathbf{u}_2\|_{\Omega_h}$, there exists a constant $C_{\mathcal{C}_\beta} > 0$ such that

$$\|\mathcal{C}_\beta(\mathbf{v}, \mathbf{u}_1) - \mathcal{C}_\beta(\mathbf{u}, \mathbf{u}_2)\|_{\Omega_h} \leq C_{\mathcal{C}_\beta} \|\mathbf{v}\|_{\Omega_h} \|\mathbf{u}_1 - \mathbf{u}_2\|_{\Omega_h} + C_{\mathcal{C}_\beta} \|\mathbf{u}_2\|_{\Omega_h} \|\mathbf{u} - \mathbf{v}\|_{\Omega_h} \tag{17}$$

where $\mathbf{u}, \mathbf{v}, \mathbf{u}_1, \mathbf{v}_1 \in H^1(\Omega_h)^3$.

- (H3), we assume $\mathcal{L}$ is a Lipschitz operator with constant $C_\mathcal{L}$. In other words, given uniform bounded $\|\mathbf{u}_1\|_{\Omega_h}$ and $\|\mathbf{u}_2\|_{\Omega_h}$, there exists a constant $C_\mathcal{L} > 0$ such that

$$\|\mathcal{L}\mathbf{u}_1 - \mathcal{L}\mathbf{u}_2\|_{\Omega_h} \leq C_\mathcal{L} \|\mathbf{u}_1 - \mathbf{u}_2\|_{\Omega_h} \tag{18}$$

where $\mathbf{u}_1, \mathbf{u}_2 \in H^1(\Omega_h)^3$.

Note that for any operator $\mathcal{H}: H^1(\Omega_h)^3 \rightarrow \mathbb{R}^3$, we define

$$\|\mathcal{H}\|_{\Omega_h} = \max\left\{\frac{\|\mathcal{H}(\mathbf{z})\|_{\Omega_h}}{\|\mathbf{z}\|_{\Omega_h}} : \mathbf{z} \in H^1(\Omega_h)^3 \quad \text{with} \quad \|\mathbf{z}\|_{\Omega_h} \neq 0\right\}. \tag{19}$$

Let us define the numerical solutions of the Crank–Nicolson method, (4) along with (5), at time $(n + 1)\triangle t$ to be $\mathbf{v}^{n+1} \in H^1(\Omega_h)^3$ and $q^{n+1/2} \in H^1(\Omega_h)$. These also satisfy the uniform boundedness hypothesis given at the beginning of this section. Our goal is to evaluate the global

error of the VCPM solutions that are approximated to Crank–Nicolson solutions. Therefore, we define the differences between the VCPM solutions and the Crank–Nicolson solutions using

$$\boldsymbol{\epsilon}^n = \mathbf{u}^n - \mathbf{v}^n \quad \text{and} \quad \eta^{n-1/2} = p^{n-1/2} - q^{n-1/2}. \tag{20}$$

Theorem 4. *We assume that* $\mathbf{mbc}^{n+1/2}$ *and* cbc^{n+1} *for all* n *have bounded discrete second-order derivatives. Under the hypotheses (H1)–(H3), global error estimates for velocity and pressure yield to second-order temporal accuracy:*

$$\left\| \boldsymbol{\epsilon}^{n+1} \right\|_{\Omega_h} = O\left(\triangle t^2 \right) \;\; and \;\; \left\| \eta^{n+1/2} \right\|_{\Omega_h} = O\left(\triangle t^2 \right).$$

Theorem 6. *If we assume the same hypothesis as in Theorem 4, the VDPM solutions converge to the VCPM solutions with second-order temporal accuracy under the same initial conditions:*

$$\left\| \boldsymbol{\epsilon}_d^n \right\|_{\Omega_h} = O\left(\triangle t^2 \right) \quad and \quad \left\| \eta_d^{n-1/2} \right\|_{\Omega_h} = O\left(\triangle t^2 \right) \tag{21}$$

for all n.

Theorems 4 and 6 along with the triangle inequality ensure that the VDPM solutions are second-order accurate in time with respect to the Crank–Nicolson solutions. Because the Crank–Nicolson method is considered to be a second-order temporal accurate method, we can conclude that the VDPM and the VCPM solutions are $O(\triangle t^2)$ of the exact solutions in a discrete l^2-norm, regardless of the formulation of the nonlinear convection term.

3   STABILITY ANALYSIS

In this paper, we assume homogenous Dirichlet or periodic boundary conditions for velocity. Therefore, $\mathbf{mbc}^{n+1/2}$ and cbc^{n+1} in (4) and (5), respectively, are identically zero. Divergence-free velocity fields are assumed to be orthogonal to the gradient fields, which may have limitations on the boundary conditions. Furthermore, $\mathcal{L}$ and $\mathcal{G}$ are commutative.

3.1   Energy estimation

Theorem 9. *Under the hypotheses (H1)–(H3), for the VCPM, there exist constants* $\tau \in \mathbb{R}^+$ *and* $B \in \mathbb{R}^+$ *such that*

$$E^{n+1} + \frac{\triangle t}{4Re} \sum_{m=0}^n \left\| \mathcal{G}\left(\mathbf{u}^{m+1} + \mathbf{u}^m \right) \right\|_{\Omega_h}^2 \le B$$

when $\triangle t \le \tau$ *for all* n. *Here,* $E^{n+1} = \frac{1}{2}\langle \mathbf{u}^{n+1}, \mathbf{u}^{n+1} \rangle_{\Omega_h}$ *denotes the kinetic energy at time level* $n+1$.

Theorem 10. *Under the hypotheses (H1)–(H3), for the VDPM, there exist constants* $\tau_d \in \mathbb{R}^+$ *and* $B_d \in \mathbb{R}^+$ *such that*

$$E_d^{n+1} + \frac{\triangle t}{4Re} \sum_{m=0}^n \left\| \mathcal{G}\left(\mathbf{u}_d^{m+1} + \mathbf{u}_d^m \right) \right\|_{\Omega_h}^2 \le B_d$$

when $\triangle t \le \tau_d$ *for all* n. *Here,* $E_d^{n+1} = \frac{1}{2}\langle \mathbf{u}_d^{n+1}, \mathbf{u}_d^{n+1} \rangle_{\Omega_h}$ *is the kinetic energy at time level* $n+1$.

3.2 von Neumann analysis

We apply the von Neumann analysis to the linearized Navier–Stokes equations in order to obtain stability diagrams that represent the distributions of the maximum magnitude of the eigenvalues of the corresponding amplification matrices.

(a) Advective, $\mathcal{C}_0$ (b) Skew-symmetric, $\mathcal{C}_{1/2}$ (c) Divergence, $\mathcal{C}_1$
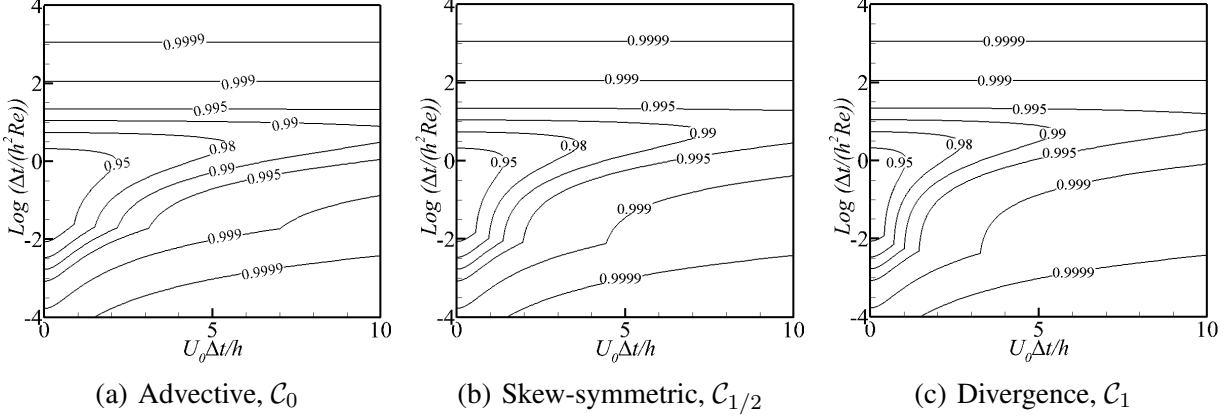
Figure 1. Distributions of the maximum magnitude of eigenvalues, $|\lambda|_{\max}$, for the VCPM along with different discrete convection operators.
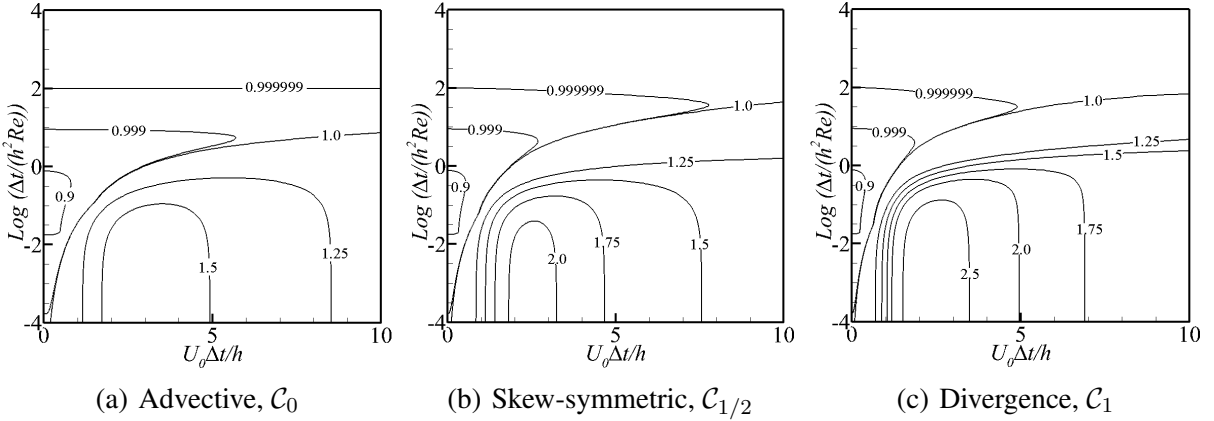

(a) Advective, $\mathcal{C}_0$ (b) Skew-symmetric, $\mathcal{C}_{1/2}$ (c) Divergence, $\mathcal{C}_1$

Figure 2. Distributions of the maximum magnitude of eigenvalues, $|\lambda_d|_{\max}$, for the VDPM along with different discrete convection operators.

4 NUMERICAL TESTS

In order to examine and compare the numerical performances of the VCPM and VDPM, as well as the semi-implicit projection method (SIPM), we consider two problems: 2D lid-driven cavity flow and periodic forced flow, which has an analytical solution.

5 CONCLUSION

We presented a mathematical study of the temporal accuracy and stability of the velocity-components decoupled projection method (VDPM) based on the time-dependent incompressible Navier–Stokes equations. We proved that decoupling procedures, such as pressure-velocity

decoupling and velocity-components decoupling, and approximated factorization procedure do not degrade the temporal accuracy. Regardless of the formulation of the nonlinear convection term, second-order accuracy of both the VCPM and VDPM in time has been achieved for both velocity and pressure. Furthermore, we analyzed the stability properties of the VCPM and VDPM using energy estimation and the von Neumann analysis that is based on fully discrete Navier–Stokes equations and linearized Navier–Stokes equations, respectively. The energy estimation indicated that both the VCPM and VDPM are stable for sufficiently small time steps, independent of the formulation of the nonlinear convection term. In addition, applying the von Neumann analysis based on linearized Navier–Stokes equations overcame the difficulties associated with the nonlinear convection term. This analysis produced stability diagrams for the stable region parameterized by the maximum magnitude of the eigenvalues of the amplification matrices. We found that the VCPM is unconditionally stable, and the eigenvalues for both the VCPM and VDPM along with $\mathcal{C}_0$ are smaller than those that use other discrete convection operators.

Numerical tests performed on the 2D lid-driven cavity flow also demonstrated that the VCPM is almost unconditionally stable and the VDPM along with $\mathcal{C}_0$ allows for a fairly large CFL number (CFL ≈ 20), indicating that the steady-state velocity distributions, as well as the time history of the velocity, agree well with references. Results for the periodic forced flow validated that both the VCPM and VDPM are second-order accurate in time, which coincides with the mathematical discussion. The computational performances of the projection methods indicate that both the VCPM and VDPM are more stable and accurate than the SIPM, and the computation time of the VDPM is more than 10 times shorter than that of the VCPM. In summary, the VDPM along with advective convection operator $\mathcal{C}_0$ is the most efficient projection method. It provides almost unconditionally stable and second-order temporal accurate numerical solutions with a computation time comparable to the SIPM.

REFERENCES

1. Kim, K., Baek, S.-J. and Sung, H. J., "An implicit velocity decoupling procedure for the incompressible Navier–Stokes equations", *International Journal for Numerical Methods in Fluids*, Vol. 38, 2002, pp. 125-138.